Boundary Circles of Mixed Phase Space, Hamiltonian Systems

Or Alus* and Shmuel Fishman†
Physics Department
Technion-Israel Institute of Technology
Haifa 3200, Israel

James D. Meiss‡
Department of Applied Mathematics
University of Colorado, Boulder,
Colorado 80309-0526 USA
(Dated: September 10, 2022)

The phase space of an area-preserving map typically contains infinitely many elliptic islands embedded in a chaotic sea. Orbits near the boundary of a chaotic region have been observed to stick for long times, strongly influencing their transport properties. The boundary is composed of invariant circles, called "boundary circles." We investigate the distribution of rotation numbers of boundary circles for the Hénon quadratic map and show that the probability of occurrence of small elements of their continued fraction expansions is larger than would be expected for a number chosen at random. However, large elements occur with probabilities distributed proportionally to the random case. These results have implications for models of transport in mixed phase space.

In almost all systems governed by classical mechanics, the phase space consists of a complex mixture of both regular and chaotic orbits [1–3]. Such dynamics, as depicted in Fig. 1, is characterized by structures on all scales. One of the most surprising consequences of this fractal structure is that a chaotic orbit will tend to "stick" to its boundary for long times [4–11]. This occurs even though a long-time average is ergodic, covering equal areas in equal times [12]. The sticking leads to an observed algebraic decay of correlation functions, Poincaré recurrences and survival times [13–15].

For the case of two degrees of freedom or equivalently, by Poincaré section, of area-preserving maps, the boundary of a chaotic region consists of infinitely many invariant circles. It is important to note that the existence of such separating circles is a generic property of smooth two-dimensional, area-preserving maps with elliptic orbits according to KAM theory [3]. These boundary circles are surrounded by leaky partial barriers, called cantori [5]. The flux of chaotic orbits through the cantori limits to zero at a boundary, explaining the observed stickiness [8]. The bottom right panel of Fig. 1 shows a resonance region surrounding a stable (elliptic) fixed point. The broken separatrix of an unstable (hyperbolic) fixed point gives rise to chaos through the famous Smale horseshoe mechanism. There is a trapped region around the stable point bounded by the circle labeled BC. Outside this circle are layers associated with periodic orbits of increasing period. Each of the stable periodic orbits in a layer gives rise to a set of islands encircling the original island. One such island, with period 7, is enlarged in the lower left panel, and it too has a boundary circle, BC'. This islands-around-islands structure is repeated on ever finer scales in repeated enlargements.

Characterization of boundary circles is the subject of the present letter. We will show that these circles are characterized by rotation numbers that have unusual continued fraction expansions, following on the pioneering study of Greene, MacKay and Stark (GMS) [16]. Although we focus on the main (class one [17]) circles, the results apply also to boundary circles on finer scales, like the (class-two) circle BC' in the figure, and can therefore be considered to be universal [18].

A boundary circle separates an outer region, where orbits can escape from the resonance, from an inner region of orbits trapped near an elliptic orbit. Though a boundary circle is isolated from the outside, every interior neighborhood typically contains other invariant circles that also encircle the elliptic point. Nevertheless, between each pair of invariant circles there are chaotic layers, as well as periodic orbits. GMS showed that the rotation number of a typical boundary circle has unusual number theoretic properties. Recall that any real number ω has a continued continued fraction expansion

$$\omega = m_0 + \cfrac{1}{m_1 + \cfrac{1}{m_2 + \ldots}} = [m_0; m_1, m_2, \ldots] \qquad (1)$$

where $m_0 \in \mathbb{Z}$ and $m_i \in \mathbb{N}$ [19]. When ω is irrational, this expansion is infinite, and a truncation after i terms gives a rational, $\omega_i = \frac{p_i}{q_i} = [m_0; m_1, m_2, \ldots, m_i]$ called the i^{th} *convergent* to ω. The convergents are alternately larger than and smaller than ω [19]. For a typical resonance, $m_0 = 0$ and the rotation number will be a decreasing function of distance from the elliptic fixed point, see the inset in Fig. 1. Equation (1) implies that $\omega_1 = \frac{1}{m_1}$ and $\omega_2 = \frac{m_2}{m_1 m_2 + 1}$ so that $\omega_1 > \omega > \omega_2$; more generally one can see that the convergents in the outer region will correspond to even i. For example, in Fig. 1,

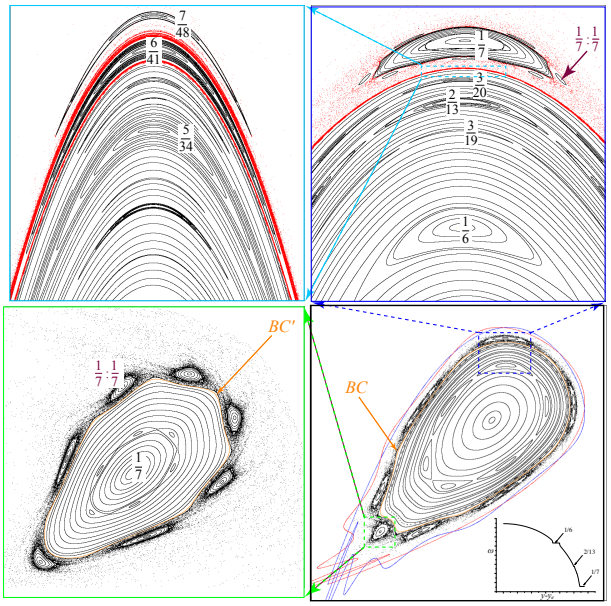

FIG. 1: Phase space of (3) for $K = -0.17197997940$ showing a hierarchy of scales. The bottom right panel shows the fixed point island and the stable (blue) and unstable (red) manifolds of the hyperbolic fixed point. An enlargement of a period-7 island is in the bottom left panel. The top right enlarges a region near the boundary circle showing the first outer approximant, $\frac{1}{7}$, to the boundary circle rotation number ω_{BC} as well as other island chains. The final zoom (top left) shows the next inner, $\frac{5}{34} = [0;6,1,4]$, and outer, $\frac{6}{41} = [0;6,1,4,1]$, approximants. Red points in the upper panels are orbits in the unbounded chaotic component.

$\omega_{BC} = [0;6,1,4,1,5,1,2,1,\ldots]$. The first convergent $\frac{p_1}{q_1} = \frac{1}{6} = [0;6]$, gives rise to a period-6 island chain in the trapped region, while the second $\frac{1}{7} = [0;6,1]$ gives a chain embedded in the outer, chaotic component. Subsequent even convergents, e.g., $\frac{6}{41} = [0;6,1,4,1]$, result in smaller islands closer to the boundary circle, see the upper left panel of the figure.

GMS computed the coefficients m_i for the rotation numbers of boundary circles and found that they differed from distribution that would occur if they were selected at random with uniform measure, namely, the Gauss-Kuzmin (GK) distribution [19],

$$p_{GK}(m) = -\log_2\left(1 - \frac{1}{(1+m)^2}\right). \qquad (2)$$

They conjectured, in contrast to (2), that for the even (outer) coefficients only the elements $m_i = 1$ and 2 occur, while for the odd (inner) coefficients only elements $m_i \leq 5$ occur.

To investigate this claim, we use Hénon's iconic area-preserving quadratic map [20]; it is a one-parameter family that can be written in the form

$$(x', y') = T(x, y) = (-y + 2K - 2x^2, x). \qquad (3)$$

We compute the rotation number of the boundary circles of the stable fixed point for a grid of 4000 K values covering the interval $(-0.25, 0.75)$. The specific question that is addressed is: How is their distribution related to (2)? The details of the algorithm will be presented elsewhere [18].

Our algorithm converged for 2667 boundary circles, and their rotation numbers are shown as a function of K in Fig. 2. The algorithm fails in two intervals of K, the largest being $(0.1920, 0.4033)$, due to bifurcations of the fixed point [18].

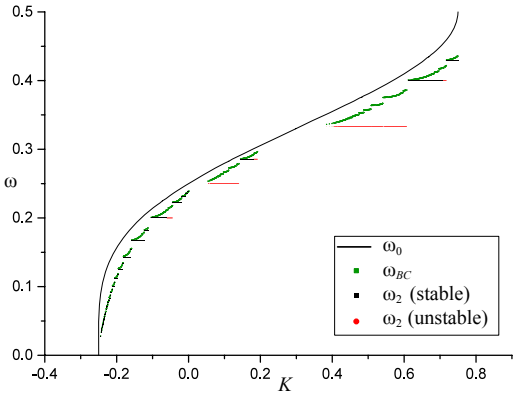

FIG. 2: Rotation numbers for (3) as a function of K. The solid curve shows the rotation number ω_0 of the elliptic fixed point, and the green points show the rotation number ω_{BC} of the class-one boundary circle. The lowest points show the rotation number ω_2 of outermost convergents to the boundary circle; black symbols denote stable and red, unstable orbits.

We explore here the distribution of the continued fraction elements, m_i, for the Hénon map (3) for a much larger sample and for longer continued fraction expansions than were computed by GMS. The empirical probability mass function, $p_{BC}(m)$, the frequency of occurrence of $m \in \mathbb{N}$ in the resulting list of coefficients m_i, is shown in Fig. 3. In the right panel of this figure, we eliminated the coefficients with $i \leq 4$, as the first few coefficients may be expected to depend on the details of the map, while the deeper approximants should be more universal. Nevertheless, the distributions are of similar nature.

The separated distributions for the inner (odd i) and outer (even i) coefficients are shown in Fig. 4. For the outer coefficients we find very few $m_i > 3$; the largest is $m = 8$. Note that both of the distributions in Fig. 4 deviate from those of GMS. In particular it appears that the inner elements are unbounded.

In Fig. 3 and Fig. 4 the results are compared with the GK distribution (2). Since the coefficients in the numerical results are bounded, $m_i \leq m_{max}$, we compare them to a conditional GK distribution $\tilde{p}_{GK}(m) = p_{GK}(m|m < m_{max}) = C p_{GK}(m)$. For our case $C \approx 1.05$ [18]. Note that our results deviate significantly from the

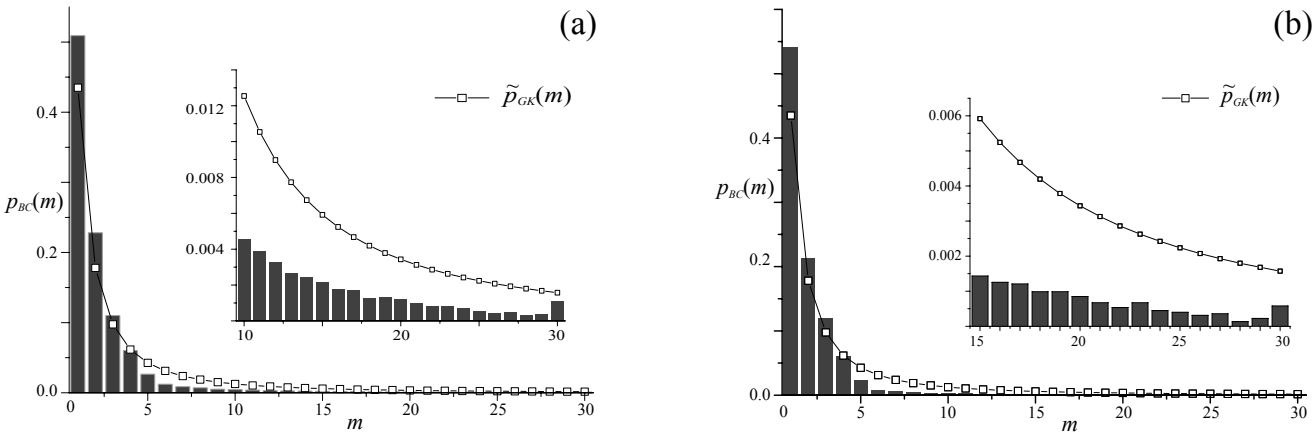

FIG. 3: Distribution of continued fraction elements for the Hénon fixed point boundary circle $K \in (-0.25, 0.75)$ compared with the conditional the GK distribution $\tilde{p}_{GK}$: (a) all coefficients and (b) those for $i > 4$.

Gauss-Kuzmin distribution for small m, but that

$$p_{BC}(m) \approx \alpha \tilde{p}_{GK}(m), \quad m > 5; \tag{4}$$

i.e., for larger m, the distribution appears to be a fixed fraction of the Gauss-Kuzmin distribution. We find $\alpha = 0.32 \pm 0.10$ for the results of Fig. 3(a) and $\alpha = 0.39 \pm 0.08$ for Fig. 4(a) while for Fig. 3(b) one finds $\alpha = 0.21 \pm 0.04$. The last value is lower since the distribution of Fig. 3(b) is distorted by the elimination of the large values of m found for $i \leq 4$.

We turn now to a heuristic explanation of our calculations. KAM theory implies that smooth, Diophantine invariant circles are structurally stable. The elements in the tail of the continued fraction for a given Diophantine number are bounded; however, the elements of a random selection of Diophantine numbers do not have a uniform bound. The outer coefficients correspond to periodic orbits on the chaotic side of the boundary circle: from this side the circle appears isolated. According to MacKay's renormalization theory [21], an isolated circle should have a "noble" rotation number, i.e., the tail beyond some position i_{max} in the continued fraction should consist of all 1's. Thus, following GMS, we expect that the outer (even i) coefficients will eventually have this property. Even the smaller i coefficients show the strong influence of the robustness of noble rotation numbers: $m_i = 1$ occurs about 85% of the time. The inner coefficients should have no such restriction: the m_i should satisfy the GK distribution. However, the small m_i coefficients are still influenced by the *nobility* of the robust circles, and so their occurrence exceeds that predicted by (2). Combining these ideas implies that distribution for the larger values of m should be a fixed fraction of the GK distribution, as (4).

In Fig. 3 and Fig. 4 the data are for the for boundary circle BC of the fixed point. If one uses data from finer scales like BC' in Fig. 1, the distributions are very similar to that in the figure [18].

In Summary: We analyzed the distribution of the elements m_i of the continued fraction for boundary circle rotation numbers and found, in contrast to the results of Greene, MacKay and Stark [16], strong evidence that the inner coefficients (odd i) are unbounded. These distributions were contrasted to the Gauss-Kuzmin (2) distribution, which applies to a uniform distribution of irrational numbers. We found that the fraction of elements taking small values is larger than expected from Gauss-Kuzmin and conversely that large elements occur with smaller probability. Moreover we conjecture that for m sufficiently large, the distribution is a fixed fraction of that expected from (2), and therefore that the continued fraction elements for the inner coefficients are unbounded. In a future paper, we will show the same property is true for different island hierarchies in the phase space as well as varying the parameter K for the map (3) [18].

Our results imply that the distribution of transport rates, used in recent hierarchical theories of the stickiness of boundary circles [13–15], should take into account this modification to the ratio of successive periods of island chains in the heirarchy, corresponding to the outer islands whose continued fractions have elements in the distribution shown in Fig. 4. To compute transport, one also requires the distribution of fluxes through the cantori between the chaotic layers; we plan to report in this in the future [18].

Acknowledgments: The work was supported in part by the Israel Science Foundation (ISF) grant number 1028/12, by the US-Israel Binational Science Foundation (BSF) grant number 2010132, by the Shlomo Kaplansky academic chair, and by National Science Foundation (NSF) grant DMS-1211350. We would like to thank Roland Ketzmerick, William Kleiber, Manual Lladser, Yoran Rozen, and Ed Ott for fruitful discussions.

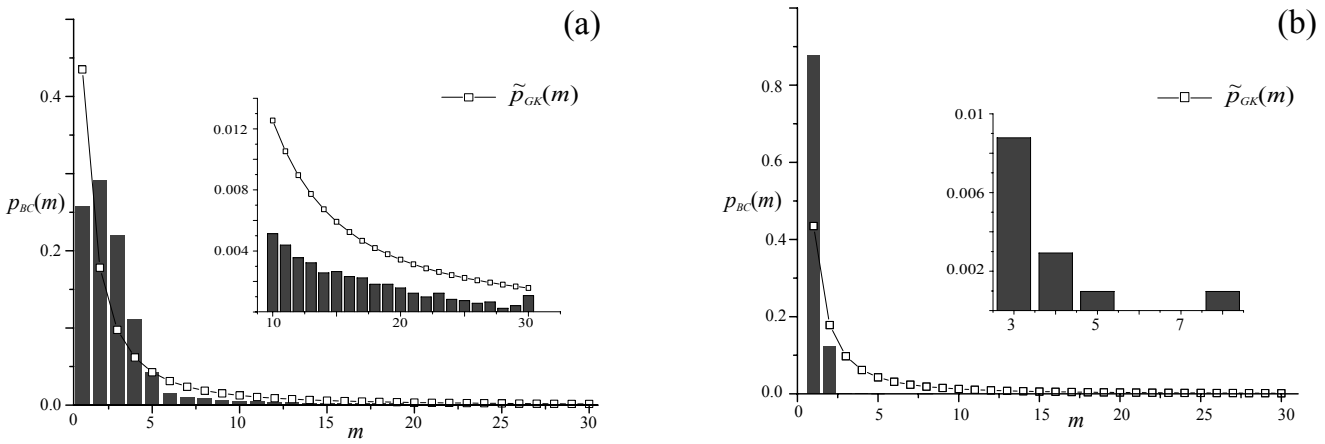

FIG. 4: Distribution of continued fraction elements of the Hénon fixed point boundary circle for $K \in (-0.25, 0.75)$ compared with the conditional distribution $\tilde{p}_{GK}$ using only elements with $i > 4$: (a) odd (inner) coefficients and (b) even (outer) coefficients.

* Electronic address: oralus@tx.technion.ac.il
† Electronic address: fishman@physics.technion.ac.il
‡ Electronic address: james.meiss@colorado.edu

[1] M.V. Berry. Regular and irregular motion. In S. Jorna, editor, *Topics in Nonlinear Dynamics*, volume 46 of *AIP Conf. Proc.*, pages 16–120. AIP, New York, 1978. URL http://dx.doi.org/10.1063/1.31417.

[2] M. Tabor. *Chaos and Integrability in Nonlinear Dynamics : an Introduction*. J. Wiley, New York, 1989. ISBN 9780471827283.

[3] J.D. Meiss. Symplectic maps, variational principles, and transport. *Rev. Mod. Phys.*, 64(3):795–848, July 1992. ISSN 0034-6861. URL http://link.aps.org/doi/10.1103/RevModPhys.64.795.

[4] C.F.F. Karney. Long-time correlations in the stochastic regime. *Physica D*, pages 360–380, 1983. URL http://www.sciencedirect.com/science/article/pii/0167278983902324.

[5] R.S. MacKay, J.D. Meiss, and I.C. Percival. Transport in Hamiltonian systems. *Physica D*, 13(1-2):55–81, August 1984. ISSN 01672789. URL http://www.mendeley.com/catalog/transport-hamiltonian-systems/.

[6] B.V. Chirikov and D.L. Shepelyansky. Correlation properties of dynamical chaos in Hamiltonian systems. *Physica D*, pages 395–400, 1984. URL http://www.sciencedirect.com/science/article/pii/0167278984901404.

[7] J.D. Hanson, J.R. Cary, and J.D. Meiss. Algebraic decay in self-similar Markov chains. *J. Stat. Phys.*, 39(3-4):327–345, May 1985. ISSN 0022-4715. URL http://link.springer.com/10.1007/BF01018666.

[8] J.D. Meiss and E. Ott. Markov tree model of transport in area-preserving maps. *Physica D*, 20(2-3):387–402, June 1986. ISSN 01672789. URL http://dx.doi.org/10.1016/0167-2789(86)90041-2.

[9] G.M. Zaslavsky, M. Edelman, and B.A. Niyazov. Self-similarity, renormalization, and phase space nonuniformity of Hamiltonian chaotic dynamics. *Chaos*, 7(1):159–181, March 1997. ISSN 1089-7682. URL http://link.aip.org/link/?CHAOEH/7/159/1.

[10] G.M. Zaslavsky and M. Edelman. Hierarchical structures in the phase space and fractional kinetics: I. Classical systems. *Chaos*, 10(1):135–146, March 2000. ISSN 1089-7682. URL http://scitation.aip.org/content/aip/journal/chaos/10/1/10.1063/1.166481.

[11] G.M. Zaslavsky. *Hamiltonian Chaos and Fractional Dynamics*. Oxford Univ. Press, Oxford, 2005.

[12] J.D. Meiss. Transient measures for the standard map. *Physica D*, 74(3 & 4):254–267, 1994. URL http://dx.doi.org/10.1016/0167-2789(94)90197-X.

[13] R. Ceder and O. Agam. Fluctuations in the relaxation dynamics of mixed chaotic systems. *Phys. Rev. E*, 87(1):012918, January 2013. ISSN 1539-3755. URL http://link.aps.org/doi/10.1103/PhysRevE.87.012918http://pre.aps.org/abstract/PRE/v87/i1/e012918.

[14] G. Cristadoro and R. Ketzmerick. Universality of algebraic decays in Hamiltonian systems. *Phys. Rev. Lett.*, 100(18):184101, May 2008. ISSN 0031-9007. URL http://link.aps.org/doi/10.1103/PhysRevLett.100.184101.

[15] R. Venegeroles. Universality of Algebraic Laws in Hamiltonian Systems. *Phys. Rev. Lett.*, 102(6):064101, February 2009. ISSN 0031-9007. URL http://link.aps.org/doi/10.1103/PhysRevLett.102.064101.

[16] J.M. Greene, R.S. MacKay, and J. Stark. Boundary circles for area-preserving maps. *Physica D*, 21(2-3):267–295, September 1986. ISSN 01672789. URL http://dx.doi.org/10.1016/0167-2789(86)90005-9.

[17] J.D. Meiss. Class Renormalization: Islands around Islands. *Phys. Rev. A*, 34(3), 1986. URL http://pra.aps.org/abstract/PRA/v34/i3/p2375_1.

[18] O. Alus, S. Fishman, and J.D. Meiss. Statistics of the Island-Around-Island Hierarchy in Hamiltonian Phase Space,2014. In preperation

[19] A.Y. Khinchin. *Continued Fractions*. University of Chicago Press, Chicago, 1964.

[20] M. Hénon. Numerical study of quadratic area-preserving mappings. *Q. J. Appl. Math.*, 27:291–312, 1969.

[21] R.S. MacKay. A renormalization approach to invariant circles in area-preserving maps. *Physica D*, 7(1-3):283–300, May 1983. ISSN 01672789. URL http://dx.doi.org/10.1016/0167-2789(83)90131-8.